

The Feasibility of Electrochemical Ammonia Synthesis in Molten LiCl-KCl Eutectics

Ian J. McPherson,^[a] Tim Sudmeier,^[a] Joshua P. Fellowes,^[a] Ian Wilkinson,^[b] Tim Hughes,^[b] S.C. Edman Tsang^{*[a]}

Abstract: Molten LiCl and related eutectic electrolytes are known to permit direct electrochemical reduction of N_2 to N^{3-} with high efficiency. It had been proposed that this could be coupled with H_2 oxidation in an electrolytic cell to produce NH_3 at ambient pressure. Here, this proposal is tested in a LiCl-KCl- Li_3N cell and is found not to be the case, as the previous assumption of the direct electrochemical oxidation of N^{3-} to NH_3 is grossly over-simplified. We find that Li_3N added to the molten electrolyte promotes the spontaneous and simultaneous chemical disproportionation of H_2 (H oxidation state 0) into H^- (H oxidation state -1) and H^+ in form of $NH_2^-/NH_2/NH_3$ (H oxidation state +1) in the absence of applied current, resulting in non-Faradaic release of NH_3 . It is further observed that NH_2^- and NH_2^- possess their own redox chemistry. However, these spontaneous reactions allow us to propose an alternative, truly catalytic cycle. By adding LiH, rather than Li_3N , N_2 can be reduced to N^{3-} while stoichiometric amounts of H^- are oxidised to H_2 . The H_2 can then react spontaneously with N^{3-} to form NH_3 , regenerating H^- and closing the catalytic cycle. Initial tests show a peak NH_3 synthesis rate of 2.4×10^{-8} mol $cm^{-2} s^{-1}$ at a maximum current efficiency of 4.2%. Isotopic labelling with $^{15}N_2$ confirms the resulting NH_3 is from catalytic N_2 reduction.

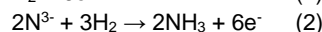
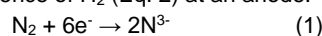
Introduction

Synthetic ammonia plays a central role in modern civilisation, accounting for as much as half of the fixed nitrogen in the terrestrial nitrogen cycle.^[1] While production on this huge scale is necessary to meet the food demands of a growing population, it comes with a correspondingly large and increasing energy requirement, consuming over 1% of the global energy supply.^[2,3] Furthermore, since this energy is currently supplied from fossil fuels, there are also significant CO_2 emissions from this process, estimated at over 1% of global CO_2 emitted in 2012.^[4] As a result, widespread efforts are underway to decrease the energy consumption of this process while developing new technologies that are compatible with renewable energy resources. Simultaneously, ammonia has begun to gain attention as a green energy vector, particularly for high capacity storage in isolated

locations. With an energy density similar to methanol, zero carbon emission on combustion and widespread storage and distribution already demonstrated by the agricultural sector, it is an attractive candidate. However, the challenge remains the de-carbonisation of its production.

Currently most ammonia is produced using the Haber-Bosch process, employing high pressures (200 bar) and an Fe catalyst to obtain equilibrium conversion of N_2 and H_2 into NH_3 .^[5] These complex plants generally operate on a very large scale, running continuously at high pressure and deriving the required H_2 from steam reforming of natural gas. However, this model is not easily converted to use renewable energy, whose wider geographic dispersion and inherent intermittency disfavour the use of large, continuous, centralised reactors. In their place a new generation of distributed, small scale, easily switched plants are envisaged whose activity can be ramped up and down to match the renewable energy supply.^[6] Holding back this vision are the difficulties in designing small yet efficient and productive reactors. The kinetics of N_2 reduction are very slow, requiring the Haber-Bosch process to operate at high temperatures. Using temperature to increase rate carries a thermodynamic penalty, however, as the equilibrium constant, K , decreases significantly from room temperature ($K(300\text{ K}) = 766$) to higher temperatures ($K(700\text{ K}) = 9.8 \times 10^{-3}$, see calculation in section S2, SI).^[5] This is compensated in the Haber-Bosch process with high reactant pressures, which itself has significant financial and energetic costs.

In contrast to thermal reactors, electrochemical cells permit the position of equilibrium to be controlled via the cell potential. If suitable redox reactions can be found, judicious control over potential enables the requirement for high pressures to be relaxed, in addition to the other benefits of electrochemical cells such as being able to control activity directly via applied voltage or current, rather than via parameters such as temperature or pressure which take much longer to change. Several electrochemical cells have been proposed for ammonia synthesis, with those based on molten salt electrolytes reporting the highest rates and current efficiencies.^[7–12] In particular, it has been reported that molten LiCl, and related eutectics, possess the fascinating ability to stabilise the N^{3-} ion and establish the reversible N_2/N^{3-} redox couple at ambient pressure.^[13–16] Ito and co-workers proposed that this could be utilised in an ammonia synthesis process, by coupling the reduction of N_2 (Eq. 1) at a cathode with its oxidation in the presence of H_2 (Eq. 2) at an anode.^[10]



They subsequently demonstrated that NH_3 was rapidly evolved from cells containing N^{3-} when H_2 , H_2O and several other H donors were added and potential was applied.^[10,17–20] Mechanistic investigation of the reaction with H_2 found that the rate of NH_3 evolution was independent of applied potential, but had a first

[a] Dr I. J. McPherson, Mr T. Sudmeier, Mr J.P. Fellowes, Prof. S.C. E. Tsang
Department of Chemistry
University of Oxford
Inorganic Chemistry Laboratory, South Parks Road, Oxford, OX1 3QR
E-mail: edman.tsang@chem.ox.ac.uk

[b] Dr I Wilkinson, Dr T Hughes
CT NTF
Siemens plc
Wharf Road, Oxford, OX29 4BP

RESEARCH ARTICLE

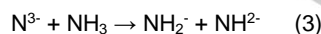
order dependence on H_2 .^[21] However, to date the ability of such cells to catalytically produce NH_3 has yet to be carefully confirmed, with only initial rates and non-catalytic conversion of N^{3-} presented.^[22]

Results and Discussion

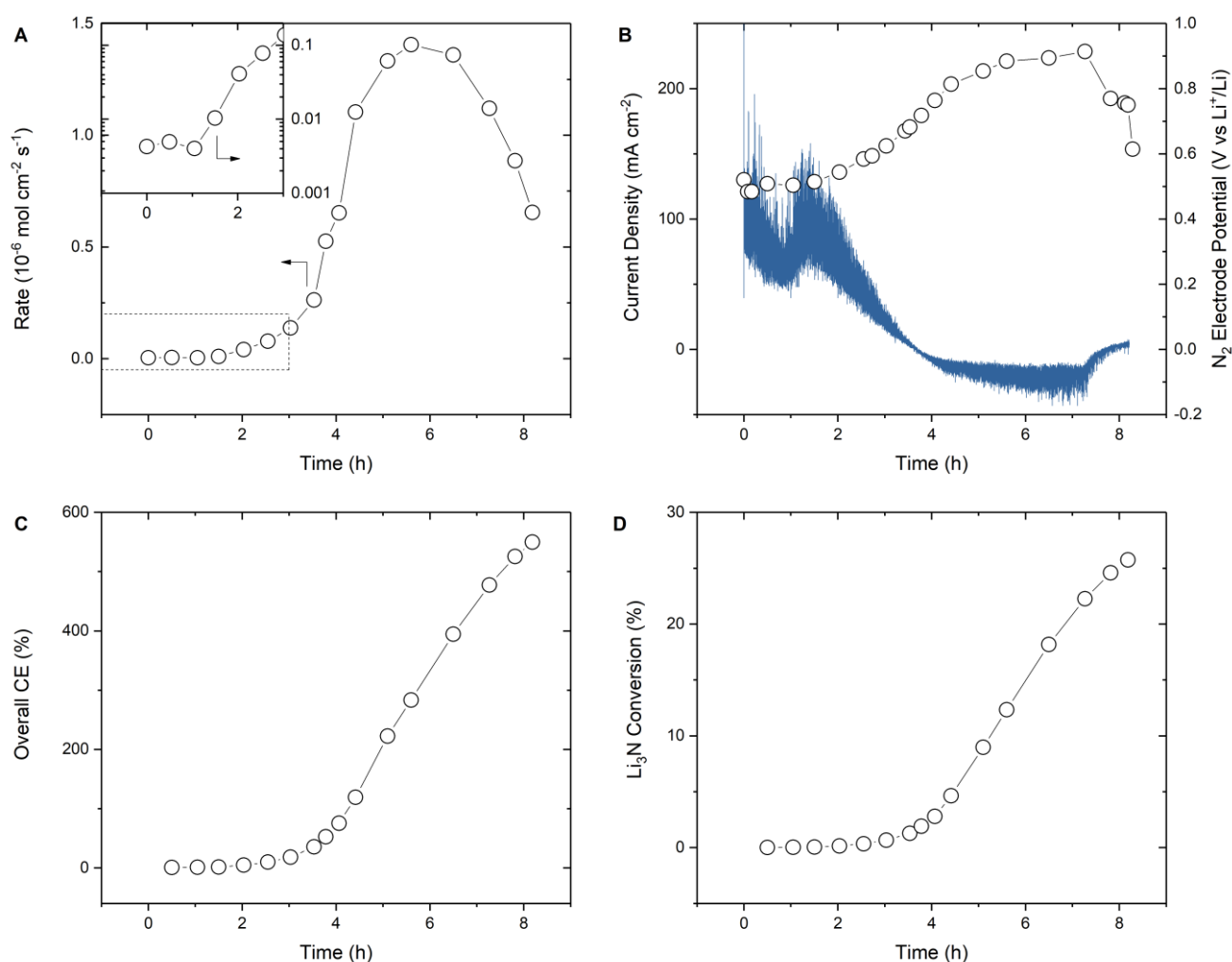
Ammonia Synthesis from Li_3N

To confirm that the cell described by Ito and co-workers^[10] is truly capable of catalytic ammonia synthesis, we reproduced their setup in which N_2 and H_2 bubbled through Ni foam electrodes into molten LiCl-KCl eutectic containing Li_3N (0.5 mol%). A potential of 0.7 V vs Li^+/Li was applied to the H_2/Ni foam working electrode in a three-electrode setup, with a Ag/AgCl electrode as the reference and the N_2/Ni foam as the counter electrode. The current, evolved NH_3 and N_2/Ni electrode potential were then sampled over the course of 8 hours (Figure 1) before the current became negligible. Over the first hour the rate of ammonia evolution is $3 \times 10^{-9} \text{ mol cm}^{-2} \text{ s}^{-1}$, identical to the rate reported

previously after 40 minutes.^[10] However, after one hour the rate begins to rise dramatically, peaking after 5.5 hours at $1.5 \times 10^{-6} \text{ mol cm}^{-2} \text{ s}^{-1}$ before falling. The delay in peak NH_3 evolution is suggested to be due to the strong absorption of NH_3 by the melt in the presence of N^{3-} , as reported previously and attributed to the reaction of NH_3 with N^{3-} to form NH_2^- and NH^{2-} species (Eq. 3).^[22]



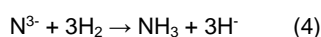
Interestingly the current seems to be inversely correlated with the rate, starting high but falling at the start of ammonia evolution, eventually becoming negative after 3.5 hours (Figure 1B, left axis). This behaviour correlates with the N_2 electrode potential, which starts off more negative than the H_2 electrode (as expected) at +0.5 V vs Li^+/Li but rises steadily to become more positive than it, reversing the polarity of the cell (Figure 1B, right axis). This reversal suggests that the composition of the electrolyte near the anode is becoming harder to oxidise, possibly a result of the depletion of N^{3-} and accumulation of NH_2^- and NH^{2-} described above.



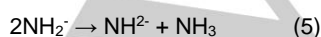
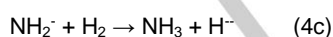
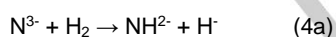
RESEARCH ARTICLE

Figure 1. Ammonia evolution under anodic potential control. H_2 electrode potential: +0.7 V vs Li^+/Li , Electrolyte: $LiCl-KCl-Li_3N$ (0.5 mol%), 723 K. Ni foam electrodes. Flow rates: H_2 (working electrode) 5 mL min^{-1} , N_2 (counter electrode) 45 mL min^{-1} , Ar (headspace) 350 mL min^{-1} . A: Ammonia evolution rate. Inset: 0-3 hours, rate on log scale. B: Current density (left), N_2 electrode potential (right). C: Cumulative current efficiency. D: Cumulative Li_3N conversion into NH_3 .

The yield of ammonia (2.5 mmol) was equivalent to conversion of only 25 mol% of the initial Li_3N (10 mmol, Figure 1C), making it impossible to determine if any N_2 reduction occurred at all (only yields greater than 100 mol% would unambiguously indicate catalysis). Furthermore, we found that the current efficiency exceeded 100%, i.e. the overall charge passed was insufficient to account for the ammonia produced (Figure 1D), revealing that the primary ammonia evolution process here is not Faradaic as originally attributed.^[23] To determine if there is any Faradaic component to ammonia evolution in this system, a control experiment was carried out under open circuit conditions (Figure 2). The initial rates are lower than seen at 0.7 V vs Li^+/Li and there is a longer delay before any increase is observed, however after 4 hours the rate does dramatically increase, reaching a peak rate again at 5.5 hours of 3.6×10^{-6} mol cm^{-2} s^{-1} before falling to negligible rates. The final yield is again equivalent to only 30% conversion of the Li_3N initially present. This behaviour is very similar to the case with applied current, although a slower onset is observed, and shows that the ammonia evolved under applied potential is not produced in a Faradaic reaction and is actually the result of a spontaneous chemical reaction between the initial dissolved Li_3N and H_2 (Eq. 4). This contrasts to the original claim of electrocatalytic N_2 reduction for ammonia production under this molten medium. Note that no NH_3 was evolved in a separate control experiment where current was applied to the $LiCl/KCl/Li_3N$ electrolyte without supplying H_2 , confirming that N^{3-} is reacting with H_2 and not residual water.



The spontaneous chemical reaction is actually very similar to the desired electrochemical oxidation reaction (Eq. 2), except the electrons from N^{3-} are used to reduce H_2 to H^- , rather than being transferred to the electrode. This reaction is spontaneous in the solid state (as the Li salts), although only slightly ($\Delta_r G = -1.15$ kJ mol^{-1}),^[24] and has been explored extensively for its role in H_2 storage, via the reversible formation of Li_2NH and $LiNH_2$.^[25] It is therefore proposed that the reaction occurs stepwise here too, via the formation of NH^{2-} and NH_2^- species (Eq. 4a-c), and/or via the bimolecular decomposition of NH_2^- (Eq. 5).



Evidence that these reactions occur in the molten state is provided by two direct observations: first, the significant H_2 partial pressure dependence of the open circuit potential; and secondly, the appearance of IR peaks in the N-H stretching region following hydrogenation. Figure 3C shows the open circuit potential of a $LiCl-KCl-Li_3N$ (0.5 mol%) melt, measured at a Ni wire, recorded as a function of $P(H_2)$ both just after H_2 was introduced, and after 20% conversion of the Li_3N to NH_3 by H_2 bubbling. There is a strong positive correlation between $P(H_2)$ and the potential, indicating not only that H_2 is involved in a potential determining equilibrium, but that it is the oxidised partner. This is consistent with the potential determining equilibrium being that between H_2 and H^- (Eq. 6), giving rise to Nernst equation (Eq. 7), where E^0 is the formal potential of the H_2/H^- couple, $P(H_2)$ is the partial pressure of H_2 and $\chi(H^-)$ the mole fraction of H^- .



$$E = E^0(H_2/H^-) + (RT/2F) \ln P(H_2)/\chi(H^-)^2 \quad (7)$$

This is further supported by the translation of the curve towards more negative potentials as the reactions proceed, consistent with an increase in H^- mole fraction. Evaluation of the slope in terms of Eq. 7 suggests the number of electrons, $n = 2.5$, close to the expected value of 2. Additional evidence for Eq. 4a-c is provided by IR spectroscopy of the melt frozen midway through reaction, where peaks are observed in the region expected for both $LiNH_2$ and Li_2NH (Figure 3D).^[26] This is also supported by recent in situ infrared experiments in which N-H stretches were observed when H_2 was bubbled through Li_3N .^[27]

The stepwise change in equilibrium potential of the H_2 electrode observed during the open circuit control measurement, and its change in polarity during the constant potential 0.7 V experiment, further suggest that the intermediates formed are themselves redox active. The redox properties of all proposed components of the electrolyte were therefore characterized to understand their interactions and determine if a truly catalytic path to ammonia synthesis in this system is indeed possible.

Voltammetric Analysis of Redox Active Species

The reactions of the proposed NH species were characterized using cyclic voltammetry, which provides characteristic potentials for the onset of redox reactions as well as insight into the reaction kinetics. In $LiCl-KCl-Li_3N$ (0.5 mol%) a series of five reversible redox couples is observed at fast scan rates (2 V s^{-1}), labelled a1/c1 to a5/c5 (Figure 3A). The a1/c1 couple ($E_{mid} = 0.19$ V, $\Delta E_p = 0.12$) is assigned to the six electron reduction of N_2 to N^{3-} (Eq. 1) having the lowest midpoint potential of all the couples, slightly more negative than the reported formal potential ($E^0 = 0.382$ V).^[28] A similar reduction peak appears when N_2 is bubbled over

RESEARCH ARTICLE

a Ni wire in pure LiCl-KCl electrolyte (Figure S2), while a slow scan of a Ni foam electrode in Li₃N (0.5 mol%) shows a linear current-potential relationship also with 0.19 V as the x intercept (Figure S3). Examination of the blank voltammogram reveals a single reduction peak around the position of c4, attributed to the

one electron reduction of residual H₂O to H₂ + OH⁻.^[29] The magnitude of this reduction current, along with a suitable estimate of the electrode area, can be used to deduce the amount of water in the melt, which is estimated to be 0.03 mol%. This non-

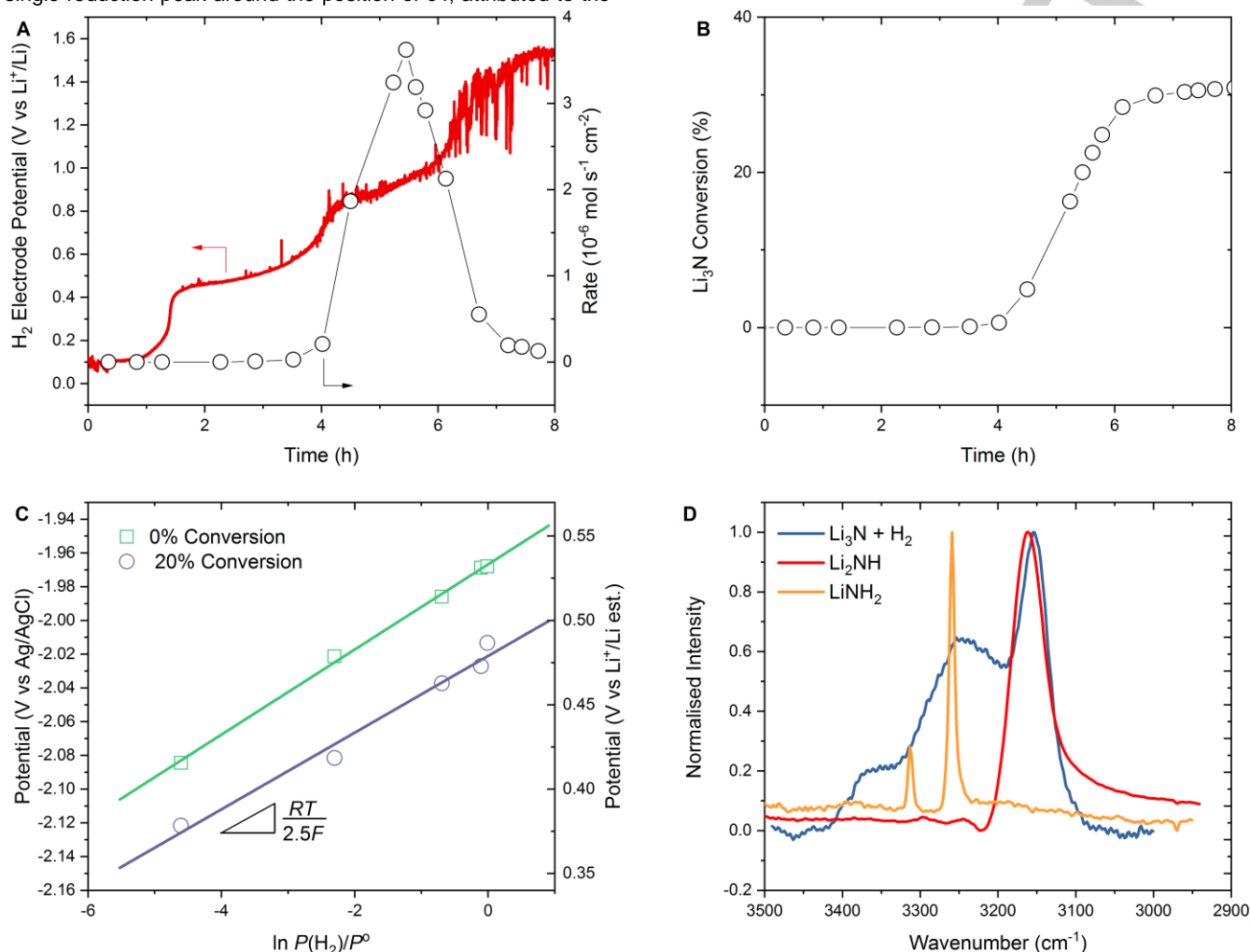
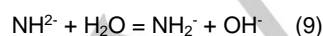
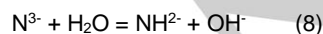


Figure 2. Ammonia evolution at open circuit. Electrolyte: LiCl-KCl-Li₃N (0.5 mol%), 723 K. Ni felt electrodes. Flow rates: H₂, 5 mL min⁻¹, N₂, 10 mL min⁻¹, Ar (headspace) 250 mL min⁻¹. A: Open circuit potential (left) and ammonia evolution rate (right). B: Conversion of initial Li₃N. C: Equilibrium potential dependence of LiCl-KCl-Li₃N (0.5 mol%) on H₂ partial pressure before and after reaction with H₂. Measured against Ag/AgCl reference electrode. D: Infrared difference spectrum in N-H stretching region of frozen LiCl-KCl-Li₃N after reaction with H₂. Li₂NH and LiNH₂ shown for reference.

negligible amount of water may react with some of the N³⁻ to generate the same protonated species as that formed via reaction with H₂ (Eq. 8,9), explaining the presence of further peaks in the voltammetry. To confirm that these species are indeed formed, voltammograms were also collected of Li₂NH, LiNH₂ and LiH.



The voltammogram of LiNH₂ at 2 V s⁻¹ (Figure 3C) consists of four pairs of peaks, aligning well with the a1/c1, a2/c2, a3/c3 and a5/c5

couples seen in Li₃N. At the slower scan rate of 100 mV s⁻¹ (Figure 3D) only a1/c1 is reversible, with c2 appearing much more significant than a2 and the a5/c5 couple replaced by a noisy limiting oxidation current. In comparison, the voltammograms of Li₂NH only shows a single clear couple (Figure 3E), aligning with a2/c2, which also appears to become irreversible at the slower scan rate (Figure 3F). The scan also shows evidence for a high potential shoulder on a2 matching the potential of the a3 peak. The onset of a new oxidation process is also observed at potentials more positive than 1.5 V. The occurrence of the a2/c2 couple in both NH₂⁻ and NH₂ is unsurprising, given that even in the absence of H₂, when LiNH₂ was added to LiCl-KCl at 723 K

RESEARCH ARTICLE

around 25 mol% was immediately evolved as NH_3 (data not shown), presumably via the reaction shown in Eq. 5, suggesting a corresponding 25 mol% is converted into NH_2^- . This suggests that measurements of LiNH_2 are actually measurements of both NH_2^- and NH^- , here in the apparent ratio 2:1.

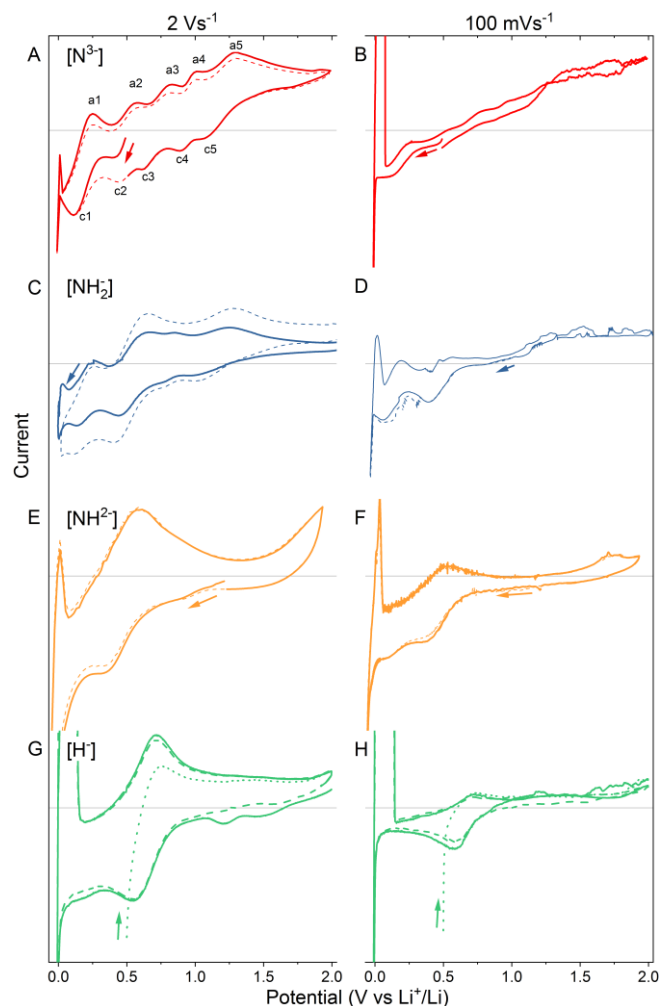
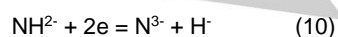
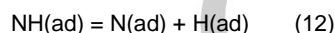
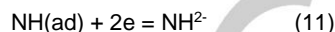


Figure 3. Cyclic voltammetry of the proposed N,H species. First (dotted/solid lines) and second (dashed lines) cycles shown. Arrows indicate starting potential and direction of scan. A,B: Li_3N (0.5 mol%), C: LiNH_2 (0.2 mol%), D: LiNH_2 (1.2 mol%), E,F: Li_2NH (1 mol%), G,H: LiH (1 mol%). A, C, E, G: scan rate: $v = 2 \text{ V s}^{-1}$, B, D, F, H: $v = 100 \text{ mV s}^{-1}$.

Focusing on the assignment of the a2/c2 couple ($E_{\text{mid}} = 0.51 \text{ V}$, $\Delta E_p = 0.12$), there are limited options for reactions of NH_2^- which could explain the irreversible reduction behaviour seen at slow scan rates in Figure 3D. One possible reduction would form N^{3-} and H^- (Eq. 10), however, based on the earlier assignment of the N_2/N^{3-} couple, N^{3-} would not be stable above 0.19 V and a net oxidation would be observed instead.

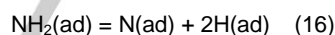
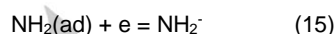


It is therefore suggested that NH_2^- is specifically adsorbed at high potential during the scan, such that current observed at a2/c2 arises from reductive desorption (Eq. 11). This can be followed by decomposition to form $\text{N}(\text{ad})$ and $\text{H}(\text{ad})$ (Eq. 12), which themselves can be reduced (Eq. 13-14), presumably at the same potentials as c1 and c3, respectively. **The production of H from NH_2^- during a2/c2 explains why the current for the non-N based a3/c3 couple is of similar magnitude to the N based processes.**



Reduction of $\text{N}(\text{ad})$ is evident in the slower scan rate scans in both NH_2^- and NH^- as a second reduction peak at the c1 position (Figure 3D,F). The much greater significance of the a1/c1 peaks in both NH_2^- scans is tentatively attributed to the more facile loss of H_2 from NH_2^- than NH^- , resulting in a lower coverage of $\text{H}(\text{ad})$ and thereby favouring reductive desorption of $\text{N}(\text{ad})$ as N^{3-} over reaction with $\text{H}(\text{ad})$ and desorption as NH_2^- .

Following the same approach, the a5/c5 couple ($E_{\text{mid}} = 1.19 \text{ V}$, $\Delta E_p = 0.20$) can be assigned to the adsorption/desorption of the NH_2^- ion (Eq. 15), with similar decomposition into $\text{N}(\text{ad})$ and $\text{H}(\text{ad})$ possible (Eq. 16).



The difference in N:H stoichiometry can also be used to explain the different behaviour seen at high potential. While two $\text{NH}(\text{ad})$ molecules must decompose (in adjacent sites) in order to evolve H_2 , giving the rate equation a quadratic dependence on NH_2^- concentration, and the requirement for neighbouring free surface sites, only one NH_2^- has to decompose to release H_2 , possibly without requiring adjacent vacant sites, making the process much faster. Thus, for the same concentration, oxidation to H_2 is likely to be much faster for NH_2^- than for NH^- . This matches well with the presence of a noisy, limiting current for NH_2^- oxidation but only a high potential current peak for NH^- oxidation.

Finally, the a3/c3 couple ($E_{\text{mid}} = 0.73 \text{ V}$, $\Delta E_p = 0.20$) is readily assigned to the H_2/H^- couple (Equation 6), based on the voltammetry of LiH (Figure 3G,H) and the previously reported midpoint potential (0.755 V at 673 K).^[30] Interestingly at slow scan rates (Figure 3H) H^- also exhibits a noisy limiting oxidation current, similar to NH_2^- , further supporting the assignment of the limiting current to H_2 evolution.

RESEARCH ARTICLE

Ammonia Synthesis from LiH

From our analysis of the original LiCl-KCl-Li₃N system we conclude that the addition of Li₃N provides a non-catalytic route to ammonia evolution, casting doubt about the feasibility of the original cell. However, our analysis also suggests that a true, alternative pathway to catalytic ammonia production does exist. If the cell can be made to reduce N₂ to N³⁻, then this should spontaneously react with H₂ gas to form ammonia and H⁻ ions. The catalytic cycle could then be closed by oxidizing the H⁻ at the anode. The desired cell reaction would then be represented by Eq. 1, Eq. 4 and Eq. 6, and is shown schematically in Figure 4. Note that it might appear more obvious to couple oxidation of H₂(g) than H⁻(sol) in this reaction, however its standard potential in LiCl-KCl is highly positive ($E^0(\text{H}_2/\text{H}^+)_{\text{calc}} = +2.610 \text{ V vs Li}^+/\text{Li}$),^[31,32] almost the same as the Ni electrode itself ($E^0 = +2.615 \text{ V}$),^[32] leading to much higher electrolysis voltages and the risk of corroding the electrode (see S4, Supporting Information).

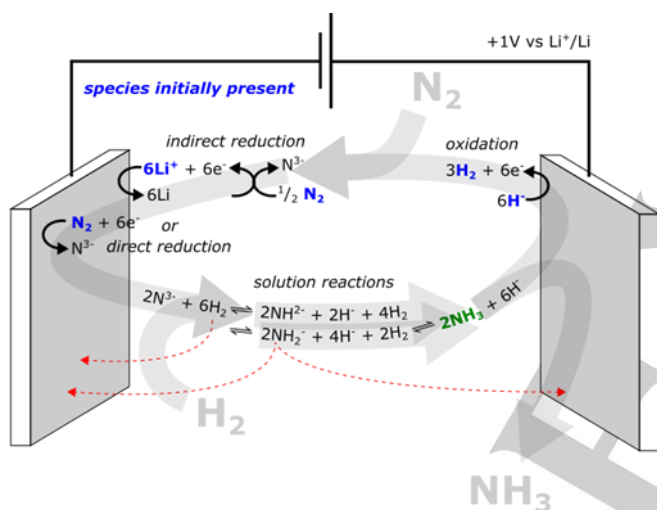


Figure 4. Catalytic cycle proposed for electrochemical NH₃ synthesis in molten LiCl-KCl-LiH. Species added to the reaction are shown in blue, remaining species in black are generated in situ, sole product NH₃ is shown in green. Red dashed lines indicate opportunities for unproductive side reactions.

We therefore setup the LiH cell to confirm catalytic ammonia production is feasible. The operating conditions were modified slightly (1 mol% LiH in place of 0.5 mol% Li₃N, 1.0 V anode potential, same gas electrodes and flow rates) and the cell tested for NH₃ synthesis activity over the course of 3 hours (Figure 5, S2 Supporting Information). Note that 1.0 V was chosen to favour productive H⁻ oxidation over unproductive reaction of NH₂⁻, based on the voltammetry (Figure 3), and LiH was added from beginning to facilitate H⁻ oxidation before the homogeneous melt reactions (Eq. 4a-c) reached steady state.

Initially very large current densities were observed, but these decreased over the course of one hour. Similar to the N³⁻ case, NH₃ evolution is not observed until after the current has

decreased (Figure 5 and Section S3, SI), presumably along with the H⁻ ion concentration, suggesting that H⁻ may also trap NH₃ via the reverse reaction of Eq. 4c. The rate of NH₃ evolution peaks at $2.8 \times 10^{-8} \text{ mol cm}^{-2} \text{ s}^{-1}$ after 2.2 hours online, which is among the highest reported rate for any electrochemical ammonia synthesis. The overall current efficiency, based on the total charge passed and the total ammonia produced, was 4.2%, while the average molar conversion of N₂ was 0.011 mol%. This can be compared to the maximum conversion of 0.006 mol% expected for purely thermal equilibrium of the gas mixture over the course of the experiment (calculations in Supporting Information, Table S4, and Figure S4).

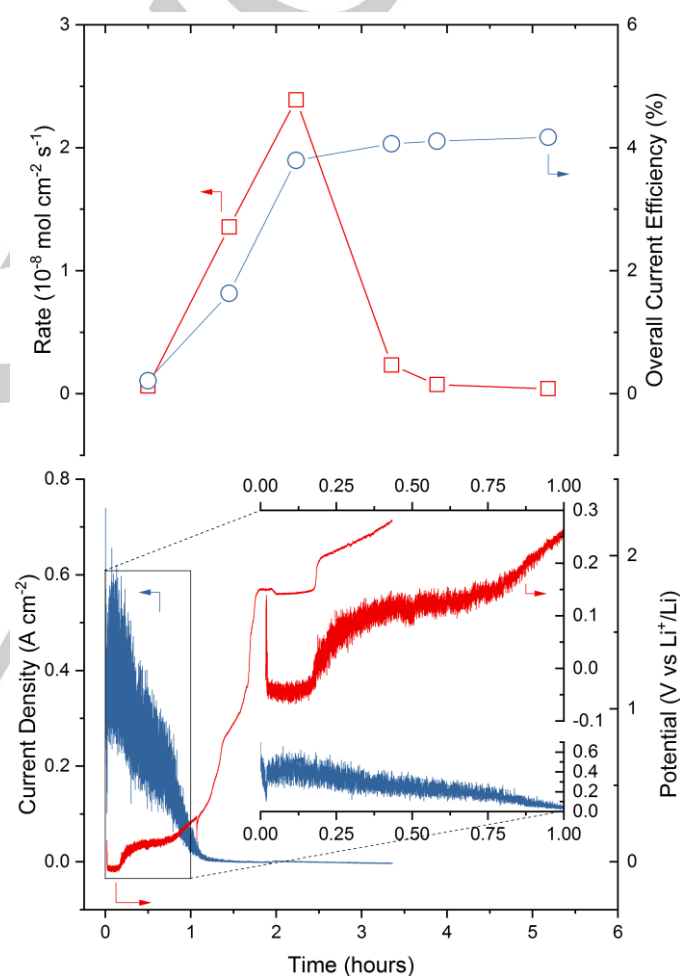


Figure 5. NH₃ synthesis results based on N₂ reduction in a LiCl-KCl-LiH (1 mol%) electrolyte. $T = 723 \text{ K}$, Flow rates: H₂ = 5 mL min⁻¹, N₂ = 45 mL min⁻¹, Ar headspace purge = 350 mL min⁻¹. Geometric electrode area = 0.126 cm². H₂ electrode potential = +1.0 V vs Li⁺/Li.

To confirm that NH₃ evolved is a result of N₂ reduction in our system rather than from an extraneous source, an isotope labelling experiment was performed (Figure 6). All conditions were maintained as in the previous LiH experiment, with the exception of the N₂ source, which was replaced with ¹⁵N₂ for

RESEARCH ARTICLE

approximately 1 hour (the contents of one cylinder), after which the source was switched back to $^{14}\text{N}_2$ for the remaining time. Very similar current densities are observed in the $^{15}\text{N}_2$ experiment (Figure 6A), along with a similar (but slightly extended) delay in NH_3 evolution. ^1H NMR spectroscopy was used to distinguish between the isotopes of NH_3 present in the trap solution, based on the different coupling between ^1H and ^{15}N ($I = \frac{1}{2}$) and ^{14}N ($I = 1$) as previously described.^[33] The NMR spectra (Figure 6B) show only the characteristic triplet of $^{14}\text{NH}_3$ in the first three time points, followed by the sudden appearance of a doublet attributed to $^{15}\text{NH}_3$, corresponding with the peak in the rate. The presence of $^{15}\text{NH}_3$ confirms that N_2 is being reduced in the reactor and thus this represents the first demonstration of truly catalytic ammonia synthesis in LiCl-KCl eutectic, i.e. without starting from Li_3N in the melt, as in previous studies.^[10,17,21]

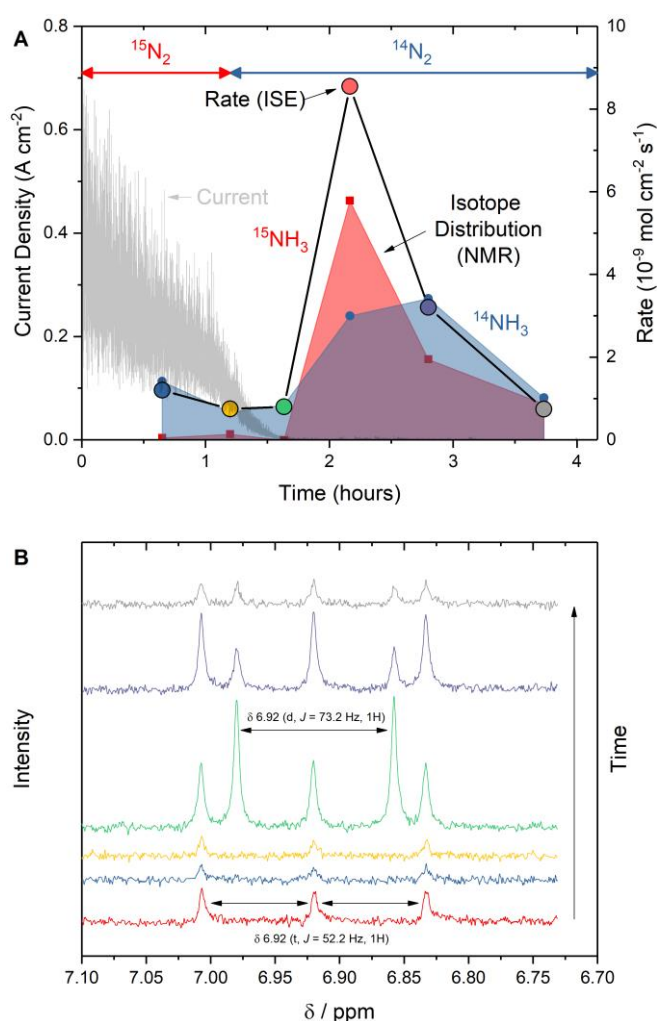


Figure 6 Isotope labelling study to confirm presence of N_2 reduction. Reaction conditions as in Figure 6, except $^{15}\text{N}_2$ was used for the first hour. A: Current (black line) NH_3 production rate determined by ISE (coloured points) and distribution of $^{15}\text{NH}_3$ and $^{14}\text{NH}_3$ produced at different times during reaction (based on the absolute values found by integrating the respective multiplet, shown in panel B, below). B: ^1H NMR spectra of the trap solutions. Spectra shown offset for clarity.

Performing the isotope experiment in this way not only provides confirmation that N_2 is being reduced in our system, but enables the origin of the decay in current and rate over time to be examined via the evolution of the $^{15}\text{NH}_3/^{14}\text{NH}_3$ product distribution. The presence of $^{14}\text{NH}_3$ at early times presumably corresponds to reduction of residual $^{14}\text{N}_2$ in the reactor or gas tubing (despite evacuating and refilling the system with Ar multiple times). Furthermore, usually the system is purged with N_2 before an experiment, allowing the melt to equilibrate before applying the voltage, however to conserve $^{15}\text{N}_2$, Ar was used to purge and the gas flow was only switched to $^{15}\text{N}_2$ just before applying the voltage. This difference may explain the slight delay in the peak rate appearing.

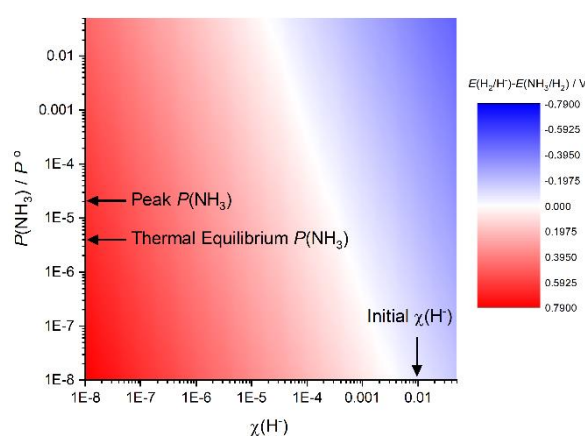
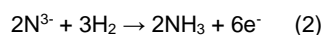


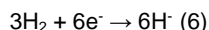
Figure 7 Reaction conditions where the hydrogenation of N^{3-} is spontaneous (red) or non-spontaneous (blue). Defined as red region where $E(\text{H}_2/\text{H}^+) - E(\text{NH}_3/\text{H}_2) > 0$. $T = 723 \text{ K}$, $\chi(\text{N}^{3-}) = 10^{-4}$, $P(\text{H}_2)/P^0 = 0.0125$.

The significant (1900 s) delay between $^{15}\text{N}_2$ flow ending and the evolution of $^{15}\text{NH}_3$ provides an estimate of the time taken for the nascent N^{3-} to react with 3H_2 to form NH_3 and leave the melt. Interestingly, there is no corresponding sharp peak for $^{14}\text{NH}_3$. This indicates that exchange of H between NH_2^- and NH_2^- is faster than the reaction between NH_2^- and H_2 , such that while it takes a long time for successive reactions of $^{15}\text{N}^{3-}$ to generate $^{15}\text{NH}_3$, later when $^{14}\text{N}^{3-}$ forms it can rapidly equilibrate with the existing $^{15}\text{NH}_2^-$ and $^{15}\text{NH}_2^-$ species, permitting $^{14}\text{NH}_3$ evolution almost immediately after switching gases.

It is clear from the behaviour of the current that the cell reactions has not yet reached the steady state as summarised in Figure 4. The reason for this becomes clear when the conditions required for the spontaneous solution reactions (4a)-(4c) to occur are considered. The H disproportionation reactions proposed to occur in the electrolyte can be separated into two half reactions:



RESEARCH ARTICLE



To be spontaneous the potential of the disproportionation reaction must be positive, i.e. $E(\text{H}_2/\text{H}^-) - E(\text{NH}_3/\text{H}_2) > 0$. This difference is calculated over a range of $P(\text{NH}_3)$ and $\chi(\text{H}^-)$ values in Figure 7. It can be seen that the H^- concentration must decrease from 1 mol% before spontaneous reaction to form NH_3 becomes possible, explaining the delay in NH_3 evolution observed. Should $P(\text{NH}_3)$ or $\chi(\text{H}^-)$ then rise significantly during operation the melt reactions become unfavourable and NH_3 evolution stops. To operate at steady state the cell must therefore be operated under closely controlled conditions. It appears from experiments in Figure 5 and 6 that conditions to achieve this steady state have not yet been found, explaining the drop in NH_3 production over time. In addition, corrosion or passivation of the Ni foam electrodes could affect the rate. Both electrodes appear black after the reaction (Figure S5), although there is no sign of NiO in the X-ray diffraction patterns of pulverised electrodes (Figure S6), just soluble NiCl_2 . The next step in the development of this cell is therefore the optimisation of the reaction conditions to maximise production of NH_3 while maintaining low concentrations of NH_3 to remain in the spontaneous regime. One way to achieve this may be by the introduction of porous membranes to separate the electrolyte at the anode, from the bulk and from that at the cathode, minimising crossover, as suggested recently.^[34]

Conclusion

From this work, we have shown that the previous assumption of direct electrochemical reaction of N_2 and H_2 in molten LiCl-KCl to form NH_3 with high efficiency is not correct. Detailed investigation into the electrochemical mechanism has revealed the existence of a number of rapid non-electrochemical reactions of N^{3-} with H_2 to form NH_3 along with NH_4^+ and NH_2^- , which are shown to be electrochemically active by cyclic voltammetry. This insight led us to propose a new, truly catalytic reaction scheme. Based on this we demonstrate electrochemical NH_3 synthesis from N_2 and H_2 at some of the highest rates yet reported, and confirm this by $^{15}\text{N}_2$ labelling. The understanding provided by this work should enable more extensive optimisation of this cell and realisation of longer term sustained electrochemical ammonia synthesis.

Experimental Section

Electrochemical experiments were carried out in a stainless steel cell mounted inside an electric furnace (Figure S1). An alumina crucible suspended from the top of the cell held the LiCl/KCl mixture (59:41 mol%, 99% Alfa Aesar), which was extensively dried before use. Gas electrodes were formed of rolled Ni foam inserted into alumina tubes, with Ni wire connections. The reference electrode was Ag/AgCl , prepared by adding AgCl (99.9%, Alfa Aesar) to LiCl-KCl (0.05 mol%) in a Pyrex tube with one end closed, and contacting the salt with a Ag wire (99.9%, Alfa Aesar). A new electrode was used for each measurement. All potentials are converted into the Li^+/Li scale by correlation with the potential of zero current in cyclic voltammograms of a Ni wire after sweeping to Li^+ reduction

potentials. The cell was operated under potentiostatic control using either a Vertex or CompactStat potentiostat (Ivium Technologies) at 723 K. Mass flow controllers supplied N_2 (99.998%, BOC) and H_2 (99.99%, BOC) to the respective electrodes, while the cell headspace was purged with Ar (99.998%, BOC). Outlet gas passed was through an acid trap containing dilute H_2SO_4 (0.01 M, 50 mL). The acid trap was changed periodically and analysed with an ion selective electrode (ThermoFisher Scientific) to determine the rate of ammonia evolution. Use of $^{15}\text{N}_2$ (98%+, CK Isotopes Ltd.) was used to confirm N_2 reduction via the presence of $^{15}\text{NH}_3$ in the acid trap, as detected by ^1H NMR spectroscopy. Further experimental details can be found in supporting information (Tables S1–S4).

Acknowledgements

This work was funded by Siemens PLC. TS acknowledges an EPSRC CASE studentship and support from a Royal Commission for the Exhibition of 1851 fellowship. N. Vranješ, A. Garzon Gonzalez, T. Adams, L. Hill and S. Davies (University of Oxford) and R. Selway (Inspired Engineering Design Ltd.) are thanked for the design and construction of equipment.

Keywords: Heterogeneous catalysis • electrochemistry • renewable resources; ammonia; nitrogen

- [1] P. M. Vitousek, J. D. Aber, R. W. Howarth, G. E. Likens, P. A. Matson, D. W. Schindler, W. H. Schlesinger, D. G. Tilman, *Ecological Applications* **1997**, 7, 737–750.
- [2] International Energy Agency, *Tracking Industrial Energy Efficiency and CO₂ Emissions*, International Energy Agency, **2007**.
- [3] International Energy Agency, Ed., *World Energy Outlook 2007*, OECD, Paris, **2007**.
- [4] T. Brown, *AMMONIA INDUSTRY* **2016**.
- [5] M. Appl, *Ammonia: Principles and Industrial Practice*, Wiley-VCH, Weinheim; Chichester, **1999**.
- [6] E. Morgan, J. Manwell, J. McGowan, *Renewable Energy* **2014**, 72, 51–61.
- [7] I. J. McPherson, T. Sudmeier, J. Fellowes, S. C. E. Tsang, *Dalton Trans.* **2019**, 48, 1562–1568.
- [8] S. Giddey, S. P. S. Badwal, A. Kulkarni, *International Journal of Hydrogen Energy* **2013**, 38, 14576–14594.
- [9] V. Kyriakou, I. Garagounis, E. Vasileiou, A. Vourros, M. Stoukides, *Catalysis Today* **2017**, 286, 2–13.
- [10] T. Murakami, T. Nishikiori, T. Nohira, Y. Ito, *J. Am. Chem. Soc.* **2003**, 125, 334–335.
- [11] S. Licht, B. Cui, B. Wang, F.-F. Li, J. Lau, S. Liu, *Science* **2014**, 345, 637–640.
- [12] J. M. McEnaney, A. R. Singh, J. A. Schwalbe, J. Kibsgaard, J. C. Lin, M. Cargnello, T. F. Jaramillo, J. K. Nørskov, *Energy Environ. Sci.* **2017**, 10, 1621–1630.
- [13] A. Bonomi, M. Hadate, C. Gentaz, *J. Electrochem. Soc.* **1977**, 124, 982–986.
- [14] A. Bonomi, M. Hadate, F. Breda, *J. Electrochem. Soc.* **1979**, 126, 248–251.
- [15] T. Goto, M. Tada, Y. Ito, *J. Electrochem. Soc.* **1997**, 144, 2271–2276.
- [16] Y. Ito, T. Goto, *Journal of Nuclear Materials* **2005**, 344, 128–135.
- [17] T. Murakami, T. Nohira, T. Goto, Y. H. Ogata, Y. Ito, *Electrochimica Acta* **2005**, 50, 5423–5426.
- [18] T. Murakami, T. Nohira, Y. Araki, T. Goto, R. Hagiwara, Y. H. Ogata, *Electrochem. Solid-State Lett.* **2007**, 10, E4–E6.
- [19] T. Murakami, T. Nohira, Y. H. Ogata, Y. Ito, *Electrochem. Solid-State Lett.* **2005**, 8, D12–D14.
- [20] T. Murakami, T. Nohira, Y. H. Ogata, Y. Ito, *J. Electrochem. Soc.* **2005**, 152, D109–D112.
- [21] T. Murakami, T. Nishikiori, T. Nohira, Y. Ito, *J. Electrochem. Soc.* **2005**, 152, D75–D78.
- [22] N. Serizawa, H. Miyashiro, K. Takei, T. Ikezumi, T. Nishikiori, Y. Ito, *J. Electrochem. Soc.* **2012**, 159, E87–E91.
- [23] Note that without the involvement of the electrode, the normalisation used is irrelevant and the units of the spontaneous rate should therefore be considered arbitrary

RESEARCH ARTICLE

- [24] C. W. Bale, E. Belise, P. Chartrand, S. A. Decterov, G. Eriksson, A. E. Gheribi, K. Hack, I. H. Jung, Y. B. Kang, J. Melancon, et al., *Calphad* **n.d.**, 54, 35–53.
- [25] P. Chen, Z. Xiong, J. Luo, J. Lin, K. L. Tan, *Nature* **2002**, 420, 302–304.
- [26] Y. Kojima, Y. Kawai, *Journal of Alloys and Compounds* **2005**, 395, 236–239.
- [27] N. Serizawa, K. Takei, T. Nishikiori, Y. Katayama, Y. Ito, *Electrochemistry* **2018**, 86, 88–91.
- [28] T. Goto, Y. Ito, *Electrochimica Acta* **1998**, 43, 3379–3384.
- [29] S. H. White, in *Ionic Liquids*, Plenum Press, New York, **1981**, p. 450.
- [30] T. Nohira, Y. Ito, *J. Electrochem. Soc.* **2002**, 149, E159–E165.
- [31] H. A. Laitinen, J. A. Plambeck, *J. Am. Chem. Soc.* **1965**, 87, 1202–1206.
- [32] H. C. Gaur, H. L. Jindal, *Electrochimica Acta* **1968**, 13, 835–842.
- [33] F. Zhou, L. Miguel Azofra, M. Ali, M. Kar, A. N. Simonov, C. McDonnell-Worth, C. Sun, X. Zhang, D. R. MacFarlane, *Energy & Environmental Science* **2017**, 10, 2516–2520.
- [34] Y. Ito, T. Nishikiori, H. Tsujimura, *Faraday Discuss.* **2016**, 190, 307–326.

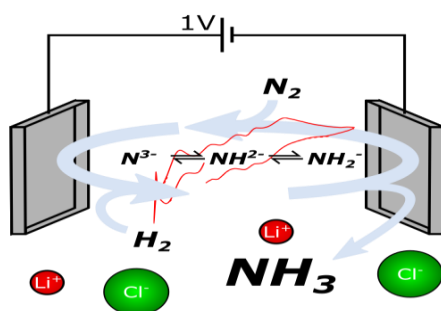
RESEARCH ARTICLE

Entry for the Table of Contents (Please choose one layout)

Layout 1:

RESEARCH ARTICLE

This work identifies the key challenges and opportunities of using molten LiCl eutectics as media for the direct electrochemical reduction of N_2 to ammonia with high efficiency.



*I.J. McPherson, T. Sudmeier, J. P. Fellowes, I. Wilkinson, T. Hughes and S.C.E. Tsang**

Page No. – Page No.

The Feasibility of Electrochemical Ammonia Synthesis in Molten LiCl-KCl Eutectics

Layout 2:

RESEARCH ARTICLE

((Insert TOC Graphic here))

*Author(s), Corresponding Author(s)**

Page No. – Page No.

Title

Text for Table of Contents